Check for updates

View Article Online
View Journal

Dalton Transactions

An international journal of inorganic chemistry

Accepted Manuscript

This article can be cited before page numbers have been issued, to do this please use: S. Tsukada, T. Abe, N. Abe, S. Nakashima, K. Yamamoto and T. Gunji, *Dalton Trans.*, 2020, DOI: 10.1039/D0DT01428A.

Dalton Transactions
An international journal of inorganic chemistry
rsc.li/dalton
Volume 46
Number 10
14 March 2017
Pages 3073-3412
ISSN 0306-0012
ROYAL SOCIETY OF CHEMISTRY
COMMUNICATION
Douglas W. Stephen *et al.*
N-Heterocyclic carbene stabilized parent sulfenyl, selenenyl, and tellurenyl cations (XH+, X = S, Se, Te)

This is an Accepted Manuscript, which has been through the Royal Society of Chemistry peer review process and has been accepted for publication.

Accepted Manuscripts are published online shortly after acceptance, before technical editing, formatting and proof reading. Using this free service, authors can make their results available to the community, in citable form, before we publish the edited article. We will replace this Accepted Manuscript with the edited and formatted Advance Article as soon as it is available.

You can find more information about Accepted Manuscripts in the Information for Authors.

Please note that technical editing may introduce minor changes to the text and/or graphics, which may alter content. The journal's standard Terms & Conditions and the Ethical guidelines still apply. In no event shall the Royal Society of Chemistry be held responsible for any errors or omissions in this Accepted Manuscript or any consequences arising from the use of any information it contains.

ROYAL SOCIETY OF CHEMISTRY

rsc.li/dalton

View Article Online
DOI: 10.1039/D0DT01428A

ARTICLE

Benzenedithiolate-bridged MoFe complexes: structures, oxidation states, and reactivities

Received 00th January 20xx,
Accepted 00th January 20xx

DOI: 10.1039/x0xx00000x

Satoru Tsukada,*[a] Takayuki Abe,[b] Naoya Abe,[b] Satoru Nakashima,[c,d] Kazuki Yamamoto,[b] and Takahiro Gunji [b]

Two benzenditholate-bridged MoFe complexes, $[(Me_3P)_2(CO)_2Mo(\mu\text{-}S_2C_6H_4)Fe(CO)_3]$ (**1**) and $[(Me_3P)(CO)_3Mo(\mu\text{-}S_2C_6H_4)Fe(CO)_3]$ (**2**), were synthesized by reacting $[Mo(S_2C_6H_4)(CO)_2(PMe_3)_2]$ (**3**) with $Fe(CO)_5$. Each complex has a direct Mo–Fe bond that is supported by a bridging benzenedithiolate ligand and a semi-bridging carbonyl ligand as elucidated by single-crystal X-ray diffractometry. The structural data and differences in reactivity of these complexes suggest that monophosphine complex **2** is formed via diphosphine complex **1**. The reaction of **2** with PMe_3 gives the diiron bis(dithiolate) complex, $[Fe(S_2C_6H_4)(CO)_2(PMe_3)]_2$ (**4**), rather than **1**. ^{57}Fe Mössbauer and X-ray photoelectron spectroscopy studies reveal the oxidation states of the metal centers in **2** to be Fe^0 and Mo^{II}.

Introduction

The chemistry of mononuclear, multinuclear, and cluster complexes of iron and other transition metal-sulfur compounds is a very active field of research because these forms are deeply embedded in the ecosystem.[1-3] Polynuclear heterometallic systems are of interest, because synergism between the different metal centers may enhance properties such as hydrogenase and nitrogenase activity. The [FeFe]- and [NiFe]-hydrogenase enzymes, which catalyze the reversible oxidation of H_2, are prominent examples.[4-6] The synthesis, properties, and catalytic mechanism of active-site models of these complexes have been investigated for many years.[7-11] Attempts to create macromolecular supports to stabilize [FeFe]-hydrogenase active-site mimetics have also been reported.[12-18]

The *R*-homocitrate-$MoFe_7S_9C$ active-site cluster of nitrogenase, which is known as FeMo-co or the FeMo-cofactor, catalyzes the reduction of dinitrogen to ammonia while releasing a molecule of H_2.[19-25] Recent model complex,[26,27] functional mimics,[28-34] biochemical,[35,36] and detailed computational[37-41] studies suggest that iron atoms are the N_2-binding sites and a central carbon atom supports the reduction of dinitrogen to ammonia. However, the mechanism of nitrogen to ammonia conversion by Mo-nitrogenase remains unclear, and the possibility that molybdenum is involved in the reduction mechanism has not been excluded.[42-45] Research on model complexes containing both molybdenum and iron is needed to further elucidate the mechanism. The $[FeMo(CO)_5(\kappa^2\text{-dppe})(\mu\text{-pdt})]$ (dppe = 1,2-bis(diphenylphosphino)ethane, pdt^{2-} = 1,3-propanedithiolate) FeMo complex was recently synthesized and characterized,[46,47] and its electronic structure, reactivity, and electrochemical behavior were investigated. To the best of our knowledge, thiolate-bridged heterobimetallic FeMo complexes scarcely have been studied[46-49] in comparison to thiolate-bridged mono- or homobimetallic complexes and of these metals[26,50,51] and sulfur-iron complexes.[28,29,31,32] Additionally, there are few methods for the synthesis of thiolate-bridged heterobimetallic FeMo complexes.[46,48,49] Recently, some dinuclear MoFe hydride complexes were synthesized as catalyst precursors of N_2 transformation.[30,33] With this in mind, the synthesis of new FeMo complexes and detailed investigation of their properties are important research objectives. Herein, we report the synthesis of two novel heterobimetallic MoFe complexes, $[(Me_3P)_2(CO)_2Mo(\mu\text{-}S_2C_6H_4)Fe(CO)_3]$ (**1**) and $[(Me_3P)(CO)_3Mo(\mu\text{-}S_2C_6H_4)Fe(CO)_3]$ (**2**), which contain a bridging 1,2-benzenedithiolate (bdt^{2-}) ligand. Structure features of both complexes are similar for bond distances and angles. The difference is the number of phosphine ligand on the Mo atom. Complex **1** has two trimethyl phosphine ligands on Mo atom. In contrast, complex **2** has one phosphine ligand, that is, one of the two phosphine ligands is replaced by carbonyl ligand. The mechanism of formation of these complexes is discussed in terms of their structures and reactivities. We also investigated the oxidation states of the metal centers in both complexes by X-ray photoelectron spectroscopy (XPS), ^{57}Fe Mössbauer spectroscopy, and electrochemical study.

Experimental

---

[a] Address here Graduate School of Engineering, Chiba University, 1-33 Yayoi-cho, Inage-ku, Chiba 263-8522, Japan. E-mail: tsukada@chiba-u.jp
[b] Department of Pure and Applied Chemistry, Faculty of Science and Technology, Tokyo University of Science, 2641 Yamazaki, Noda, Chiba 278-8510, Japan
[c] Graduate School of Science, Hiroshima University, 1-4-1 Kagamiyama, Higashi-Hiroshima, 739-8527, Japan
[d] Natural Science Centre for Basic Research and Development, Hiroshima University, 1-4-1 Kagamiyama, Higashi-Hiroshima, 739-8527, Japan

† Electronic Supplementary Information (ESI) available. CCDC 1853085-1853087. For ESI and crystallographic data in CIF or other electronic format see DOI: 10.1039/x0xx00000x

View Article Online
DOI: 10.1039/D0DT01428A

General

All reactions and recrystallizations were carried out under an argon atmosphere. Silica-gel column chromatography was carried out under air for all reactions. Tetrahydrofuran was purchased from Kanto Chemical (Tokyo, Japan), distilled from sodium, dried over 4Å molecular sieves, and degassed with nitrogen prior to use. Pentacarbonyliron, iodomethane, and magnesium turnings were purchased from Kanto Chemical. Trimethylamine *N*-oxide, triphenyl phosphite, and dibutyl ether were purchased from Sigma-Aldrich Japan. Column chromatography was performed using Wako gel C-200 (spherical, neutral; FUJUFILM Wako Pure Chemicals). $[Mo(S_2C_6H_4)(CO)_2(PMe_3)_2]$ was prepared according to the literature method.[52]

NMR spectra were recorded on a JEOL ECP-500 (500 MHz) spectrometer. ^1H NMR (500 MHz) and $^{13}C\{H\}$ NMR (126 MHz) spectra were recorded using tetramethylsilane as an internal standard. $^{31}P\{^1H\}$ NMR (202 MHz) spectra were recorded using 85% phosphoric acid as an external standard. IR spectra were recorded on a JASCO FT-IR 6100 spectrometer, and UV-Vis-near infrared (NIR) spectra were recorded on a JASCO V670 spectrometer. Uncorrected melting points were determined using a Bibby Stuart Scientific SMP3 instrument. HR-ESI mass spectra were recorded on a JEOL JMS-T100CS AccuTOF CS spectrometer. Elemental analyses were carried out using a Perkin Elmer 2400II CHNS/O analyzer. All XPS spectra were recorded with a Shimadzu ESCA-3400 instrument and were calibrated against the C1s peak at 285.0 eV.

Synthesis of $[(Me_3P)_2(CO)_2Mo(\mu\text{-}S_2C_6H_4)Fe(CO)_3]$ (1) and $[(Me_3P)(CO)_3Mo(\mu\text{-}S_2C_6H_4)Fe(CO)_3]$ (2).

$Fe(CO)_5$ (0.540 mL, 4.0 mmol) was added to a solution of $[Mo(S_2C_6H_4)(CO)_2(PMe_3)_2]$ (**3**), 0.888 g, 2.0 mmol) and Me_3NO (0.300 g, 4 mmol) in THF (80 mL) at 0 °C. The mixture was stirred for 3 h and then concentrated under reduced pressure. The residue was purified by silica-gel column chromatography with dichloromethane/hexane (1:5, v/v) as the eluent. The orange first fraction was collected and evaporated to give $Fe_2(bdt)(CO)_6$ (0.092 g, 11%) as an orange powder. The red second fraction was collected and evaporated to give $[Fe(S_2C_6H_4)(CO)_2(PMe_3)]_2$ (**4**, 0.125 g, crude yield 10%) as a red powder. The green fourth fraction was collected and evaporated to give **2** (0.151 g, 14%) as a dark green powder, which was recrystallized from $CDCl_3$/hexane at –30 °C to give black single crystals suitable for X-ray crystallography. The third fraction contained $[Mo(S_2C_6H_4)(CO)_2(PMe_3)_2]$ (**3**) and **1**. This fraction was evaporated, and the resulting residue was purified by silica-gel column chromatography with THF/hexane (1:6, v/v) as the eluent. The green first fraction was collected and evaporated to give **1** (0.185 g, 16%) as a green powder. Single crystals of **1** suitable for X-ray crystallography were obtained by a method identical to that used for preparing crystals of **2**. The second reddish-brown fraction was collected and evaporated to recover $[Mo(S_2C_6H_4)(CO)_2(PMe_3)_2]$ (**3**, 0.424 g, crude yield 48%) as a reddish-brown powder.

1: mp 137.0–138.0 °C. ^1H NMR (500 MHz, $CDCl_3$) δ 1.44 (br s, 18H, PMe_3), 6.58 (br s, 2H, Ar-H), 7.16 (br s, 2H, Ar-H). $^{13}C\{H\}$ NMR (126 MHz, $CDCl_3$) δ 20.1 (s, PMe_3), 124.9 (s), 128.5, 151.4, 209.2. $^{31}P\{H\}$ NMR (202 MHz, $CDCl_3$) δ –0.5 (s). IR (KBr pellet, cm^{-1}) ν = 3056, 2974, 2911, 2046, 1975, 1876, 1803, 1428, 948, 743, 673, 321, 590, 558. HRMS (ESI-TOF, positive), *m/z* calcd. for $C_{17}H_{22}FeMoO_5P_2S_2Na$ 608.86851 $[M+Na]^+$; found 608.86724. Anal. Calcd. for $C_{17}H_{22}FeMoO_5P_2S_2$: C, 34.95; H, 3.80. Found: C, 34.65; H, 3.65.

2: mp 159.0–160.0 °C (decomp.). ^1H NMR (500 MHz, $CDCl_3$) δ 1.39 (d, $J_{H\text{-}P}$ = 9.0 Hz, 9H, PMe_3), 6.67 (dd, J = 3.5, 5.5 Hz, 2H, Ar-H), 7.24 (dd, J = 3.5, 5.5 Hz, 2H, Ar-H). $^{13}C\{H\}$ NMR (126 MHz, $CDCl_3$) δ 18.4 (d, $J_{C\text{-}P}$ = 26.0 Hz, PMe_3), 125.6 (s), 129.1, 150.4 (d, $J_{C\text{-}P}$ = 3.9 Hz), 205.8, 208.3. $^{31}P\{H\}$ NMR (202 MHz, $CDCl_3$) δ –10 (s). IR (KBr pellet, cm^{-1}) ν = 2975, 2911, 2063, 1992, 1970, 1907, 1869, 1439, 1419, 1287, 954, 749, 614, 584. HRMS (ESI-TOF, positive), *m/z* calcd. for $C_{15}H_{13}FeMoO_6PS_2Na$ 560.81923 $[M+Na]^+$; found 560.82031. Anal. Calcd. for $C_{15}H_{13}FeMoO_6PS_2$: C, 33.60; H, 2.44. Found: C, 33.51; H, 2.27.

Reaction of 1 with CO

Complex **1** (0.056 g, 0.1 mmol) in dichloromethane (5 mL) was stirred under an atmosphere of CO at room temperature for 24 h. The CO was replaced with Ar, and the mixture was concentrated under reduced pressure. The crude product was purified by silica-gel column chromatography with dichloromethane/hexane (1:6, v/v) as the eluent. The green first fraction was collected and evaporated to give **2** (0.016 g, 29%) as a green powder. The red sixth fraction was collected and evaporated to give **3** (0.020 g, 44%) as a red-brown powder.

Synthesis of PMe_3

PMe_3 was synthesized by a slight modification of a previous method.[53] Because PMe_3 is malodorous, its synthesis was conducted with exhaust ventilation.

Iodomethane (37.4 mL, 0.60 mol) was added slowly in a dropwise manner to a mixture of magnesium metal (15 g, 0.60 mol) and dibutyl ether (100 mL). When the flask began to warm, the remaining iodomethane was diluted with dibutyl ether (50 mL) and added to the mixture so that gentle reflux was maintained. After the preparation of the Grignard reagent, triphenyl phosphite (39 mL, 0.15 mol) was added slowly to the mixture. When the flask began to warm, the remaining triphenyl phosphite was diluted with dibutyl ether (50 mL) and added to the mixture, which was cooled to 0 °C. The gray-green solution that formed following the addition of triphenyl phosphite was distilled at 160 °C to give the crude product as a colorless liquid. Redistillation of the crude product at 40 °C gave PMe_3 (2.3 g, 21%) as a colorless liquid.

Reaction of 1 with PMe_3

PMe_3 (0.103 mL, 1.0 mmol) was added to a solution of **1** (0.058 g, 0.1 mmol) in THF (5 mL), and the mixture was stirred at room temperature for 3 h. After evaporation of the mixture, the crude product was purified by silica-gel column chromatography with THF/hexane (1:6, v/v) as the eluent. The first red fraction was

View Article Online
DOI: 10.1039/D0DT01428A

collected and evaporated to give $[Fe(S_2C_6H_4)(CO)_2(PMe_3)]_2$ (**4**, 0.058 g, 88% of Fe converted) as a red powder. mp 132.8–133.5 °C (decomp.). **4**: ^1H NMR (500 MHz, $CDCl_3$) δ 1.45 (br s, 18H, PMe_3), 6.69 (br s, 4H, Ar-H), 7.19 (br s, 4H, Ar-H). $^{13}C\{H\}$ NMR (126 MHz, $CDCl_3$) δ 14.5 (s, PMe_3), 122.1 (s), 128.4, 146.8, 211.3. $^{31}P\{H\}$ NMR (202 MHz, $CDCl_3$) δ 9 (s). IR (KBr pellet, cm^{-1}) ν = 3050, 2973, 2906, 2002, 1946, 1443, 1416, 1282, 942, 856, 736, 670, 632, 599, 560. HRMS (ESI-TOF, positive), *m/z* calcd. for $C_{15}H_{13}FeMoO_6PS_2Na$ 678.87857 $[M+Na]^+$; found 678.87700. Anal. calcd. for $C_{22}H_{26}Fe_2O_4P_2S_4$: C, 40.26; H, 3.99; S, 19.54. Found: C, 40.22; H, 4.03; S,19.58.

Reaction of 2 with PMe_3

PMe_3 (0.103 mL, 1.0 mmol) was added to a solution of **2** (0.054 g, 0.1 mmol) in THF (5 mL), and the mixture was stirred at room temperature for 3 h. After evaporation of the mixture, the crude product was purified by silica-gel column chromatography with THF/hexane (1:6, v/v) as the eluent. The first red fraction was collected and evaporated to give $[Fe(S_2C_6H_4)(CO)_2(PMe_3)]_2$ (**4**, 0.062 g, 94% of Fe converted) as a red powder. The red powder was recrystallized from $CDCl_3$/hexane at –30 °C to give single crystals suitable for X-ray crystallography.

Reaction of 2 with CO

The reaction was carried out in the same manner as described for the reaction of **1** with CO. **2** was recovered quantitatively at the end of the reaction.

Reaction of 1 with acetonitrile

Complex **1** (0.019 g, 0.03 mmol) in acetonitrile (2 mL) was stirred at reflux for 7.5 h. The solution was evaporated after consumption of **1** as determined by TLC. A brown powder was obtained, which proved to be a complex mixture.

Reaction of 2 with acetonitrile

Complex **2** (0.016 g, 0.03 mmol) in acetonitrile (2 mL) was stirred at reflux for 7.5 h. Evaporation of the solvent provided **2**, which was recovered in quantitative yield indicating that no reaction occurred.

Reaction of 1 with hydrazine monohydrate

Hydrazine monohydrate (49 μL, 1.0 mmol) was added to a solution of **1** (0.056 g, 0.1 mmol) in THF (5 mL), and the mixture was stirred at room temperature for 24 h. After evaporation of solvent, the crude product was purified by silica-gel column chromatography with THF/hexane (1:6, v/v) as the eluent. The red first fraction was collected and evaporated to give **4** (0.030 g, 45%). The green second fraction was collected and evaporated to recover **1** (0.022 g, 41%).

Reaction of 2 with hydrazine monohydrate

The reaction was carried out in the same manner as described for the reaction of **1** with hydrazine monohydrate. The red first fraction was separated by silica-gel column chromatography with THF/hexane (1:6, v/v) as the eluent and was collected and evaporated to give **4** (0.041 g, 61%).

X-ray Diffractometry

Single-crystal XRD data were collected using a Bruker AXS SMART APEX CCD X-ray diffractometer equipped with a monochromatic Mo K_α radiation (0.7107 Å) source. Empirical absorption corrections using equivalent reflections and Lorentzian polarization corrections were applied using the SADABS program.[54] All data were collected using the SMART and Bruker SAINTPLUS (Version 6.45) software packages. Structures were solved using the SHELXA-97 program[55] and refined against F^2 using SHELEXL-97.[56]

^{57}Fe Mössbauer spectroscopy

A $^{57}Co(Rh)$ source moving in constant acceleration mode was used for ^{57}Fe Mössbauer spectroscopy. ^{57}Fe Mössbauer spectra at room temperature and 78 K were obtained using a Wissel Mössbauer spectrometer and a proportional counter. Mössbauer parameters were obtained by least-squares fitting to Lorentzian peaks. The spectra were calibrated against the six lines of α-Fe, the center of which was taken as the zero isomer shift.

Electrochemistry

Cyclic voltammetry was performed with a BAS ALS 650E electrochemical analyzer. The n-Bu_4NClO_4 supporting electrolyte was recrystallized from EtOH and dried under vacuum for 24 h. Measurements were carried out under an argon atmosphere in a three-electrode cell (BAS Inc.) using a 3-mm diameter glassy carbon working electrode (BAS Inc.), a Pt wire counter electrode, and an Ag/$AgClO_4$ reference electrode (0.01 M $AgClO_4$ in 0.1 M Bu_4NClO_4/acetonitrile, BAS Inc.). Ferrocene was added as an internal standard after each measurement. Caution: Bu_4NClO_4 is a potentially explosive chemical.

Results and discussion

Synthesis and stability of the MoFe complexes

The reaction of the mononuclear molybdenum-dithiolene complex, $[Mo(S_2C_6H_4)(CO)_2(PMe_3)_2]$ (**3**), with $Fe(CO)_5$ and Me_3NO in THF gave the heterobimetallic MoFe diphosphine complex **1** and monophosphine complex **2** (Scheme 1). The combination of $Fe(CO)_5$ and Me_3NO generates a reactive $[Fe(CO)_4]$ fragment.[57] **1** and **2** are not produced if the reaction is carried out in the absence of Me_3NO. Diphosphine complex **1** gradually decomposes in the air in solution and the solid-state as indicated by a dark green to red-brown color change. The red-brown degradation product

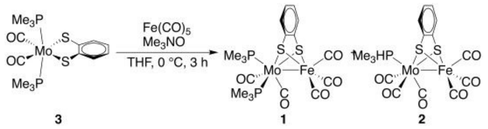

Scheme 1 Synthesis of MoFe complexes **1** and **2**.

View Article Online
DOI: 10.1039/D0DT01428A

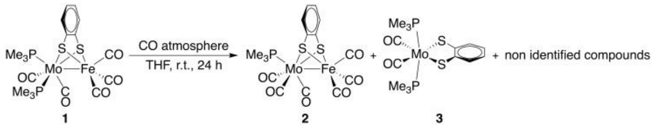

Scheme 3 Reaction of **1** in an atmosphere of CO.

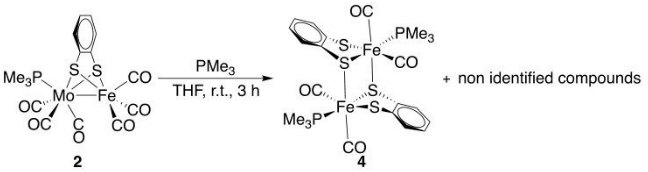

Scheme 2 Reaction of **2** with PMe$_3$.

could not be identified. Complex **1** does not decompose for several months when stored in an inert atmosphere in the solid-state. Monophosphine complex **2** is more stable, which does not decompose even after a year in an inert atmosphere in the solid-state and persists in the air for a few days in solution and the solid-state. Complex **1** is soluble in tetrahydrofuran, dichloromethane, chloroform, acetone, and toluene. Complex **2** is soluble in hexane in addition to the above solvent.

Reactivities of 1 and 2

The mechanisms for the formation of **1** and **2** were explored by investigating the reactivities of the complexes. We first reacted **1** with CO gas in CH_2Cl_2 and obtained **2** (29%) and **3** (44%) after stirring for 24 h (Scheme 2). However, the reaction of **2** with PMe$_3$ gave the diiron bis(dithiolate) complex **4** rather than **1** in almost quantitative yield (Scheme 3). The reaction occurred quickly following the addition of PMe$_3$ and was accompanied by a solution color change from the green of **2** to the red of **4**. Complex **1** was not formed in the reaction. The results indicate that **2** is generated from **1** during the formation of the MoFe complexes. Alternatively, **2** could be formed from **3** using Fe(CO)$_5$ and Me$_3$NO; either PMe$_3$ or carbonyl ligand must be eliminated from Mo atom before **2** is formed (see Scheme 4). If the PMe$_3$ is eliminated, **2** generate without going through **1**. Complex **4** is stable in an argon atmosphere but decomposes in a solution exposed to air within 30 min accompanied by a red-to-green color change. Complex **4** was also obtained by the reaction of **1** with PMe$_3$.

Despite their similar structures (see below), **1** and **2** exhibit differences in reactivity. Acetonitrile, which is known to react with bimetallic pdt-bridged MoFe complexes,[47] was investigated first. Complex **1** reacts with acetonitrile to give a complicated mixture of products, which could not be identified. ^{1}H NMR and IR spectra of the mixture are shown in Figures S15 and S16 in the supporting information. Complex **2** is unreactive toward acetonitrile and CO gas.

Reactions of **1** and **2** with hydrazine monohydrate, which often is used to probe the reactivity of Fe-Mo bimetallic complexes that model the active site of nitrogenase, also were investigated.[29,31] Reaction of **1** with hydrazine monohydrate gives **4** in 45% yield with 41% recovery of unreacted **1**.

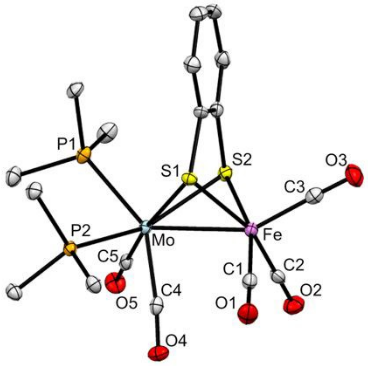

Fig. 1 ORTEP drawings of **1** with thermal ellipsoids at the 50% probability level. Hydrogen atoms are omitted for clarity. Selected bond lengths (Å), intramolecular distances (Å), and bond angles (°): Mo–Fe 2.6885(6), C1–O1 1.137(4), Fe–C1 1.794(4), C2–O2 1.142(4), Fe–C2 1.787(4), C3–O3 1.130(4), Fe–C3 1.816(4), C4–O4 1.163(4), Mo–C4 1.959(3), C5–O5 1.165(4), Mo–C5 1.949(3), Fe–C4 2.986(3), Fe–C5 4.007(3), Mo–P1 2.5274(9), Mo–P2 2.4696(9), Fe–C1–O1 178.9(3), Fe–C2–O2 177.6(3), Fe–C3–O3 178.7(3), Mo–C4–O4 172.1(3), Mo–C5–O5 178.9(3).

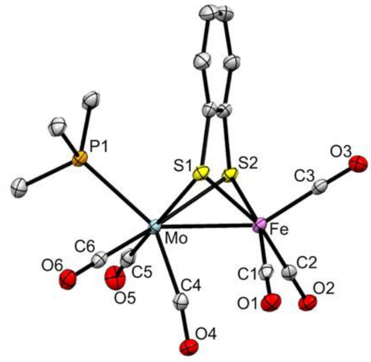

Fig. 2 ORTEP drawings of **2** with thermal ellipsoids at the 50% probability level. Hydrogen atoms are omitted for clarity. Selected bond lengths (Å), intramolecular distances (Å), and bond angles (°): Mo–Fe 2.6936(4), C1–O1 1.135(3), Fe–C1 1.805(2), C2–O2 1.132(3), Fe–C2 1.804(2), C3–O3 1.140(3), Fe–C3 1.805(2), C4–O4 1.156(3), Mo–C4 1.973(2), C5–O5 1.149(3), Mo–C5 1.984(3), C6–O6 1.146(3), Mo–C6 1.996(2), Fe–C4 2.784(2), Fe–C5 4.110(3), Mo–P1 2.5356(6), Fe–C1–O1 177.9(2), Fe–C2–O2 179.4(2), Fe–C3–O3 178.3(2), Mo–C4–O4 170.7(2), Mo–C5–O5 176.3(2), Mo–C6–O6 179.0(2).

Complex**2** reacts with hydrazine monohydrate to provide **4** in 61% yield with the concomitant disappearance of **2** from the reaction mixture. In MoFe-co, hydrazine and diazene are both reduced to ammonia by the wild-type nitrogenase.[41] On the other hand, the reaction of **1** and **2** with hydrazine showed different and interesting reactivity from MoFe-co. The molybdenum part in both **1** and **2** seem to eliminate easily under the reaction with a nucleophile such as PMe$_3$ and hydrazine monohydrate. The difference of reactivity among **1**, **2**, and MoFe-co indicate that the coordination states and the oxidation states around metals of these compounds are different. the coordination states and the oxidation states are considered important for the generation of ammonia in FeMo-co.

Crystal structures

View Article Online
DOI: 10.1039/D0DT01428A

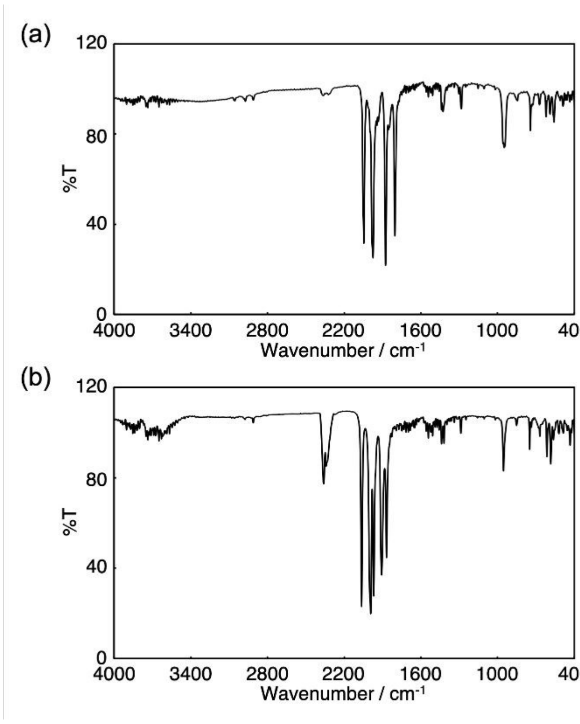

Fig. 3 IR spectra of (a) **1** and (b) **2** as KBr pellets.

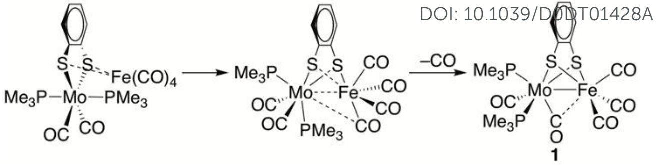

Scheme 4 Mechanism for the reaction of **3** with a reactive [Fe(CO)$_4$] fragment.

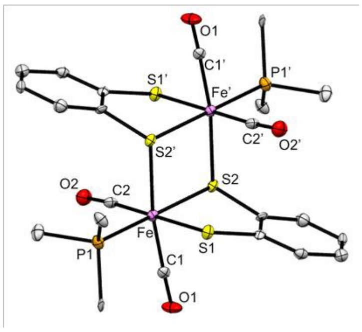

Fig. 4 ORTEP drawing of **4** with thermal ellipsoids at the 50% probability level. Hydrogen atoms are omitted for clarity.

The molecular structures of **1** and **2** were determined by single-crystal X-ray diffractometry (Figures 1 and 2). Around the Fe atom of both complexes show slightly distorted octahedral geometry. The C1–O1 and C2–O2 carbonyl ligands are located on the *trans* position to sulfur atoms. The C3–O3 carbonyl ligand and Mo atom are in *trans* position. On the other hand, around the Mo atom of both complexes show seven coordinated capped octahedral geometry. The C4–O4 carbonyl ligand is located on the *trans* position to P1 phosphine ligand. In complex **1**, the C5–O5 carbonyl ligand and P2 phosphine ligand are placed on the *trans* position to sulfur atoms. The P2 phosphine ligand is replaced by the C6–O6 carbonyl ligand in **2**. The Mo–Fe distances in **1** (2.6885(6) Å) and **2** (2.6936(4) Å) are shorter than in the pdt-bridged Mo–Fe bimetallic complex (2.7795(8) Å).[46] These distances also are shorter than the sum of the covalent radii (Mo: 1.54 Å, Fe: 1.52 Å).[58] Thus, **1** and **2** contain a Mo–Fe bond that is supported by a bridging benzenedithiolate ligand. The molybdenum–dithiolene plane of starting material **3** is absent in these structures. The Mo–C4–O4 bond angle in **1** and **2** is smaller than the other metal–C–O bond angles in these compounds. Furthermore, the Fe–C4 distance is much shorter than the Fe–C5 distance. The C4–O groups in both **1** and **2** were classified as semi-bridging but closer to terminal, according to an analysis of the asymmetric parameter α (α (**1**) = 0.52 and α (**2**) = 0.41).[59,60] The IR spectra also supported the above assignment. The IR spectra of **1** and **2** exhibit two strong bands (**1**: 1803 and 1876 cm^{-1}, **2**: 1869 and 1907 cm^{-1}) with other strong bands at 1900–2000 cm^{-1} that are assigned to the terminal carbonyl groups (Figure 3). The pair of strong bands is assigned to semi-bridging coordination modes (asymmetric and symmetric vibrations).[61] These results indicate that the coordination mode of the C4–O4 carbonyl group is semi-bridging with a weak bonding interaction between the C4 atom and the Fe atom in each complex. This feature supports the notion that the Mo and Fe atoms provide π-bonding back-donation.

The ligand positions about the Mo center in **1** differ from those in the starting material **3**, wherein the two PMe$_3$ ligands occupy apical positions, and the benzenedithiolate and two carbonyl ligands occupy equatorial positions. Both PMe$_3$ ligands are located on the same plane in **1**. Scheme 4 shows a proposed reaction mechanism based on the changes in PMe$_3$ positions upon moving from **3** to **1** and the semi-bridging carbonyl ligand configuration in **1**. An active Fe(CO)$_4$ species, generated by the reaction of Fe(CO)$_5$ with Me$_3$NO, begins by interacting with the benzenedithiolate S atoms and Mo center in **3**. One of the carbonyl carbons on the Fe center establishes an interaction with the Mo atom, after which it moves to the Mo center while maintaining its interaction with Fe. One carbonyl ligand on Mo is eliminated as carbon monoxide, and the PMe$_3$ ligand close to the Fe-containing moiety moves to the position previously occupied by the eliminated CO. This establishes the observed stereochemistry of the PMe$_3$–Mo–PMe$_3$ unit in **1**. Similar CO ligand-transfer reactions have been reported for dithiolate-bridged dimetal complexes.[62]

Figure 4 shows the crystal structure of **4**. The three Fe–S bonds are almost equal in length [Fe-S1: 2.326(2) Å, Fe-S2: 2.297(2) Å, Fe-S2': 2.341(2) Å], and the Fe–Fe distance (3.441(2) Å) indicates a lack of bonding interaction between the metals. These facts indicate that each iron atom enjoys six-coordinate octahedral geometry consisting of two sulfur atoms from one benzendithiolate ligand, two carbonyl ligands, one phosphine

View Article Online
DOI: 10.1039/D0DT01428A

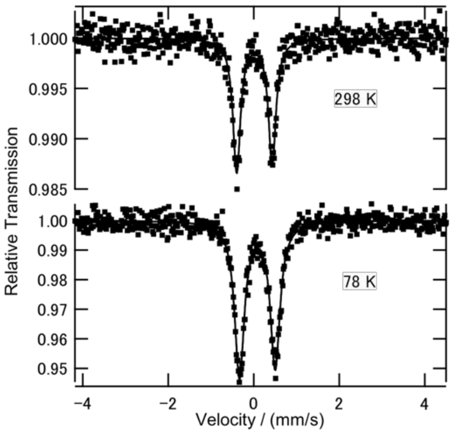

Fig. 5 ^{57}Fe Mössbauer spectra of solid **2** at 298 K (top) and 78 K (bottom). The black dots are raw data, and the solid lines are least-squares fits to the spectral data.

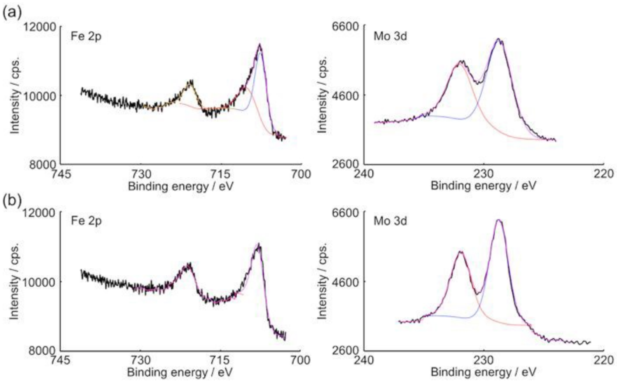

Fig. 6 X-ray photoelectron spectra of (a) **1** and (b) **2**.

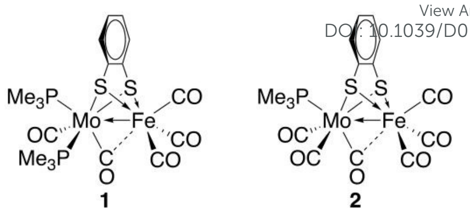

Fig. 7 Coordination mode of **1** and **2**.

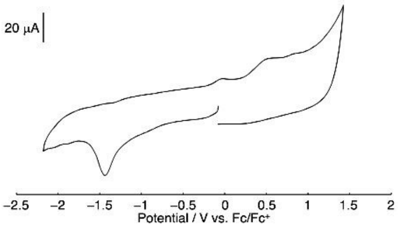

Fig. 8 Cyclic voltammogram of **2** (0.5 mM) at 0.1 V s^{-1} in 0.1 M *n*-Bu_4NClO_4/CH_2Cl_2.

ligand, and one sulfur atom from the other dithiolene ring. The dithiolene rings have lost planarity. The dihedral angle between the S1–C–C–S2 plane and the S1–Fe–S2 plane is 27.10°. This shared sulfur-atom structure is known for some half-sandwich dithiolene complexes, such as $[C_6Me_6Co(S_2C_6H_4)]_2$[63] and $[C_6Me_6Rh(S_2C_6H_4)]_2$,[64] in which the dinuclear Co and Rh complexes are converted into mononuclear species in solution and in the solid-state.[63,64] In contrast, **4** exhibits a dinuclear structure under both solution conditions.

Oxidation states of metal centers

Metal oxidation states in **2** were investigated by ^{57}Fe Mössbauer spectroscopy at 298 K and 78 K (Figure 5). Complex **2** exhibits a doublet with an isomer shift (δ) of 0.02 mm/s and a quadrupole splitting (ΔE_q) of 0.84 mm/s at 298 K. These values are largely unchanged when the sample is cooled to 78 K (δ = 0.08 mm/s, ΔE_q = 0.83 mm/s), which suggests that the oxidation state and geometry of the Fe center are temperature-independent. The δ-value of **2** differs from that of the propanedithiolate-bridged $Fe^{II}Mo^0$ complex, $[FeMo(CO)_5(\kappa^2\text{-dppe})(\mu\text{-pdt})]$ (δ = 0.20 mm/s),[46] which contains an Fe–Mo bond. This value also differs from those of the sulfido-bridged $Fe^{III}Mo^V$ monodithiolene oxomolybdenum complex, $[Ph_4P]_2[(PhS)_2FeS_2MoO(tdt)]\bullet CH_3CN\bullet Et_2O$ (tdt^{2-} = toluenedithiolate) (δ = 0.25 ± 0.01 mm/s),[65] Fe^{II}-Mo^{VI}-S cluster complexes (δ =0.50–0.63 mm/s),[66] and Fe^{II}/Fe^{III}-Mo^{VI}-S cluster complexes (δ = 0.41–0.49 mm/s).[67] The δ-values of $[Mo^{IV}{}_2Fe^{II}{}_2]$-hydride clusters,[30] $\{(C_5Me_5)Mo(PMe_3)\}_2\{FeN(SiMe_3)_2\}_2(H)_8$ (δ = 0.748(1) mm/s), $\{(C_5Me_5)Mo(PMe_3)\}_2\{Fe(SR)\}_2(H)_8$ (R = 2,4,6-*i*$Pr_3C_6H_2$) (δ = 0.707(2) mm/s), and dinuclear [MoFe]-hydride complexes, $(C_5Me_5)Mo^{II}(PMe_3)(H)_2(CN\textit{t}Bu)_2Fe^{II}\{N(SiMe_3)_2\}$ (δ = 0.667(2) mm/s),[30] $[(C_5Me_5)Mo^{IV}(PMe_3)(THF)(\mu\text{-}H)_3Fe^{II}(C_5Me_5)][B(C_6F_5)_4]$ (δ = 0.281(2) mm/s),[33] $(C_5Me_5)Mo^{II}(PMe_3)(\mu\text{-}H)(\mu\text{-}PPh_2)Fe^{II}(C_5Me_5)$ (δ = 0.359(2) mm/s),[33] differ from that of **2**. The δ-value of **2** is close to that of the Fe^0 center in $Fe(CO)_5$ (0.009 mm/s)[68] and the $[\textit{cis}\text{-}Fe(InX_3)_2(CO)_4]^{2-}$ moiety in $[Fe(NCMe)_6][\textit{cis}\text{-}Fe(InX_3)_2(CO)_4]$ (X = Cl, Br, I) (–0.03 mm/s).[69] The XPS spectrum of **2** exhibits peaks at 708.1 and 721.3 eV, which correspond to the Fe $2p_{3/2}$ and $2p_{1/2}$ binding energies, respectively (Figure 6b).[70] These binding energies are lower than those of the *p*-alkynylbenzeneazadithiolate Fe(I)-Fe(I) complex (710.9 and 724.5 eV).[71] The Fe $2p_{3/2}$ binding energy of **2** also is close to that of Fe metal, which occurs near 707 eV.[70] The Mo $3d_{5/2}$ and $3d_{3/2}$ binding energies of **2** occur at 228.8 and 232.0 eV, respectively. These values are almost identical to those of **3** (229.0 and 232.1 eV), which is a Mo(II) complex (Figure S17).

The ^{57}Fe Mössbauer and XPS results suggest that the formal oxidation states of the metal centers in **2** are Fe(0) and Mo(II). The Fe and Mo binding energies of **1** (Fe: 707.9 and 720.9 eV, Mo: 228.8 and 232.0 eV) are almost the same as those of **2** (Figure 6a). Thus, the formal oxidation states of the metal centers in **1** also are Fe(0) and Mo(II).

Based on the oxidation state of Fe and Mo atoms and crystal structures in **1** and **2**, the coordination modes of both complexes are shown in Figure 7. The Fe atom is acting as a two-electron donor to the Mo atom. Additionally, the sulfur atoms in this oxidation state approximation have negative charges to balance Mo(II), and therefore have a dative bond to the Fe atom as two-electron donors. The semi-bridging carbonyl ligand is acting as a π-acceptor from the Fe atom.

The cyclic voltammogram of **2** shows an irreversible reduction peak at $E_p^{red} = -1.44$ V (Figure 8). The reduced form of **2** is unstable and decomposes. This reduction process differs considerably from that of $[FeMo(CO)_5(\kappa^2\text{-dppe})(\mu\text{-pdt})]$[47] and dithiolate-bridged diiron complexes such as $[Fe_2(\mu\text{-}S_2C_6H_4)(CO)_6]$.[72-74] $[FeMo(CO)_5(\kappa^2\text{-dppe})(\mu\text{-pdt})]$ exhibits reversible or partially reversible redox behavior.[47] The diiron complex shows a single reversible reduction in CH_2Cl_2 that corresponds to a two-electron transfer.[72] The reduced forms of some multinuclear dithiolate-bridged complexes are known to be stabilized by the cleavage of Fe–S bonds and/or a change in the coordination mode of their carbonyl ligands.[61,73] However, the reduced form of **2** is not stabilized by the presence of benzenedithiolate or carbonyl ligands.

Conclusions

We have synthesized the benzendithiolate-bridged MoFe complexes **1** and **2** by reacting **3** with $Fe(CO)_5$ in combination with Et_3NO. Each complex contains a Mo–Fe bond that is supported by a bridging benzenedithiolate ligand and one semi-bridging carbonyl ligand. Based on crystal-structure and reactivity data for **1** and **2**, we propose a mechanism for the generation of each complex. The semi-bridging carbonyl group, which is thought to be derived from the $Fe(CO)_4$ fragment, plays a central role in the generation of **2** from **1**. Mechanistic details of the generation of **2** are not revealed. ^{57}Fe Mössbauer spectroscopy and XPS indicate that the formal oxidation states of the metal centers in **1** and **2** are Fe(0) and Mo(II). Electrochemistry shows that the reduced form of **2** is unstable. These results are expected to lead to new polynuclear heterometallic complexes such as active site models of enzymes. Especially, investigation of properties of metal atoms of thiolate-bridged heterobimetallic FeMo complexes **1** and **2** may one of the keys to unlocking the reaction mechanism of the nitrogenase. Further investigations into the detailed electrochemical properties of **2**, such as electrochemical proton reduction, are currently underway.

Conflicts of interest

There are no conflicts to declare.

Acknowledgements

This work was supported by a Grant-in-Aid for Scientific Research on Innovative Area "New Polymeric Materials Based on Element-Blocks (No.2401)" (24102008A02) from The Ministry of Education, Culture, Sports, Science, and Technology, Japan. This work was supported by JSPS KAKENHI Grant Number JP16K17951 and JP19K15637.

Notes and references

1. B. Krebs and G. Henkel, *Angew. Chem. Int. Ed.*, 1991, **30**, 769-788.
2. R. H. Holm and W. Lo, *Chem. Rev.*, 2016, **116**, 13685-13713.
3. S. Ohta and Y. Ohki, *Coord. Chem. Rev.*, 2017, **338**, 207-225.
4. J. C. Fontecilla-Camps, A. Volbeda, C. Cavazza and Y. Nicolet, *Chem. Rev.*, 2007, **107**, 4273-4303.
5. A. L. De Lacey, V. M. Fernández, M. Rousset and R. Cammack, *Chem. Rev.*, 2007, **107**, 4304-4330.
6. W. Lubitz, E. Reijerse and M. van Gastel, *Chem. Rev.*, 2007, **107**, 4331-4365.
7. G. A. N. Felton, C. A. Mebi, B. J. Petro, A. K. Vannucci, D. H. Evans, R. S. Glass and D. L. Lichtenberger, *J. Organomet. Chem.*, 2009, **694**, 2681-2699.
8. F. Gloaguen and T. B. Rauchfuss, *Chem. Soc. Rev.*, 2009, **38**, 100-108.
9. C. Tard and C. J. Pickett, *Chem. Rev.*, 2009, **109**, 2245-2274.
10. D. Schilter, J. M. Camara, M. T. Huynh, S. Hammes-Schiffer and T. B. Rauchfuss, *Chem. Rev.*, 2016, **116**, 8693-8749.
11. S. Ogo, *Coord. Chem. Rev.*, 2017, **334**, 43-53.
12. C. Zhan, X. Wang, Z. Wei, D. J. Evans, X. Ru, X. Zeng and X. Liu, *Dalton Trans.*, 2010, **39**, 11255-11262.
13. D. Heine, C. Pietsch, U. S. Schubert and W. Weigand, *J. Polym. Sci., Part A: Polym. Chem.*, 2013, **51**, 2171-2180.
14. C. A. Tooley, S. Pazicni and E. B. Berda, *Polym. Chem.*, 2015, **6**, 7646-7651.
15. X. Zhu, W. Zhong and X. Liu, *Int. J. Hydrogen Energy*, 2016, **41**, 14068-14078.
16. W. P. Brezinski, M. Karayilan, K. E. Clary, K. C. McCleary-Petersen, L. Fu, K. Matyjaszewski, D. H. Evans, D. L. Lichtenberger, R. S. Glass and J. Pyun, *ACS Macro Lett.*, 2018, **7**, 1383-1387.
17. W. P. Brezinski, M. Karayilan, K. E. Clary, N. G. Pavlopoulos, S. Li, L. Fu, K. Matyjaszewski, D. H. Evans, R. S. Glass, D. L. Lichtenberger and J. Pyun, *Angew. Chem. Int. Ed. Engl.*, 2018, **57**, 11898-11902.
18. M. Karayilan, W. P. Brezinski, K. E. Clary, D. L. Lichtenberger, R. S. Glass and J. Pyun, *Angew. Chem. Int. Ed. Engl.*, 2019, **58**, 7537-7550.
19. B. K. Burgess and D. J. Lowe, *Chem. Rev.*, 1996, **96**, 2983-3012.
20. R. N. F. Thorneley and D. J. Lowe, *J. Biol. Inorg. Chem.*, 1996, **1**, 576-580.
21. T. Spatzal, M. Aksoyoglu, L. Zhang, S. L. Andrade, E. Schleicher, S. Weber, D. C. Rees and O. Einsle, *Science*, 2011, **334**, 940.
22. K. M. Lancaster, M. Roemelt, P. Ettenhuber, Y. Hu, M. W. Ribbe, F. Neese, U. Bergmann and S. DeBeer, *Science*, 2011, **334**, 974-977.
23. Y. Hu and M. W. Ribbe, *J. Biol. Inorg. Chem.*, 2014, **19**, 731-736.
24. O. Einsle, *J. Biol. Inorg. Chem.*, 2014, **19**, 737-745.
25. Y. Hu and M. W. Ribbe, *J. Biol. Inorg. Chem.*, 2015, **20**, 435-445.
26. Y. Li, Y. Li, B. Wang, Y. Luo, D. Yang, P. Tong, J. Zhao, L. Luo, Y. Zhou, S. Chen, F. Cheng and J. Qu, *Nat. Chem.*, 2013, **5**, 320-326.
27. M. A. Kaczmarek, A. Malhotra, G. A. Balan, A. Timmins and S. P. de Visser, *Chem. Eur. J.*, 2018, **24**, 5293-5302.
28. I. Coric, B. Q. Mercado, E. Bill, D. J. Vinyard and P. L. Holland, *Nature*, 2015, **526**, 96-99.

29. S. E. Creutz and J. C. Peters, *J. Am. Chem. Soc.*, 2015, **137**, 7310-7313.
30. Y. Ohki, Y. Araki, M. Tada and Y. Sakai, *Chem. Eur. J.*, 2017, **23**, 13240-13248.
31. D. E. DeRosha, V. G. Chilkuri, C. Van Stappen, E. Bill, B. Q. Mercado, S. DeBeer, F. Neese and P. L. Holland, *Nat. Chem.*, 2019, **11**, 1019-1025.
32. A. L. Speelman, I. Coric, C. Van Stappen, S. DeBeer, B. Q. Mercado and P. L. Holland, *J. Am. Chem. Soc.*, 2019, **141**, 13148-13157.
33. K. Ishihara, Y. Araki, M. Tada, T. Takayama, Y. Sakai, W. M. C. Sameera and Y. Ohki, *Chem. Eur. J.*, 2020, DOI: 10.1002/chem.202000104.
34. C. H. Arnett and T. Agapie, *J. Am. Chem. Soc.*, 2020, DOI: 10.1021/jacs.0c01896.
35. L. C. Seefeldt, B. M. Hoffman and D. R. Dean, *Curr. Opin. Chem. Biol.*, 2012, **16**, 19-25.
36. B. M. Hoffman, D. Lukoyanov, D. R. Dean and L. C. Seefeldt, *Acc. Chem. Res.*, 2013, **46**, 587-595.
37. I. Dance, *Chem. Commun.*, 2013, **49**, 10893-10907.
38. I. Dance, *Dalton Trans.*, 2015, **44**, 18167-18186.
39. J. B. Varley, Y. Wang, K. Chan, F. Studt and J. K. Norskov, *Phys. Chem. Chem. Phys.*, 2015, **17**, 29541-29547.
40. P. E. Siegbahn, *J. Am. Chem. Soc.*, 2016, **138**, 10485-10495.
41. L. Rao, X. Xu and C. Adamo, *ACS Catal.*, 2016, **6**, 1567-1577.
42. B. E. Smith, M. C. Durrant, S. A. Fairhurst, C. A. Gormal, K. L. C. Grönberg, R. A. Henderson, S. K. Ibrahim, T. Le Gall and C. J. Pickett, *Coord. Chem. Rev.*, 1999, **185-186**, 669-687.
43. M. C. Durrant, *Biochemistry*, 2002, **41**, 13934-13945.
44. L. C. Seefeldt, I. G. Dance and D. R. Dean, *Biochemistry*, 2004, **43**, 1401-1409.
45. R. Bjornsson, F. Neese, R. R. Schrock, O. Einsle and S. DeBeer, *J. Biol. Inorg. Chem.*, 2015, **20**, 447-460.
46. S. Bouchard, M. Clemancey, G. Blondin, M. Bruschi, K. Charreteur, L. De Gioia, C. Le Roy, F. Y. Petillon, P. Schollhammer and J. Talarmin, *Inorg. Chem.*, 2014, **53**, 11345-11347.
47. S. Bouchard, M. Bruschi, L. De Gioia, C. Le Roy, F. Y. Petillon, P. Schollhammer and J. Talarmin, *Inorg. Chem.*, 2019, **58**, 679-694.
48. T. A. Cross, M. H. Frey and S. J. Opella, *J. Am. Chem. Soc.*, 1983, **105**, 7471-7473.
49. L. D. Rosenhein and P. E. Fanwick, *J. Organomet. Chem.*, 1992, **431**, 327-333.
50. D. Yang, Y. Li, B. Wang, X. Zhao, L. Su, S. Chen, P. Tong, Y. Luo and J. Qu, *Inorg. Chem.*, 2015, **54**, 10243-10249.
51. D. Yang, S. Xu, Y. Zhang, Y. Li, Y. Li, B. Wang and J. Qu, *Inorg. Chem.*, 2018, **57**, 15198-15204.
52. S. Tsukada, N. Abe and T. Gunji, *Polyhedron*, 2016, **117**, 73-79.
53. M. L. Luetkens, A. P. Sattelberger, H. H. Murray, J. D. Basil, J. P. Fackler, R. A. Jones and D. E. Heaton, in *Inorg. Synth.*, John Wiley & Sons, Inc., 2007, pp. 305-310.
54. G. M. Sheldrick, *SADABS (V2.10)*; Program for Siemens area detector absorption correction; University of Göttingen: Göttingen, Germany, 1996.
55. G. M. Sheldrick, *SHELXS–97 (6.14 8/06/00)*; Program for Crystal Structure Solution; University of Göttingen: Göttingen, Germany, 1996.
56. G. M. Sheldrick, *SHELXS–97 (6.14 8/06/00)*; Program for Crystal Structure Refinement; University of Göttingen: Göttingen, Germany, 1996.
57. Y. Shvo and E. Hazum, *J. Chem. Soc., Chem. Commun.*, 1975, 829-830.
58. B. Cordero, V. Gomez, A. E. Platero-Prats, M. Reves, J. Echeverria, E. Cremades, F. Barragan and S. Alvarez, *Dalton Trans.*, 2008, 2832-2838.
59. M. D. Curtis, K. R. Han and W. M. Butler, *Inorg. Chem.*, 1980, **19**, 2096-2101.
60. R. H. Crabtree and M. Lavin, *Inorg. Chem.*, 1986, **25**, 805-812.
61. S. Muratsugu, K. Sodeyama, F. Kitamura, S. Tsukada, M. Tada, S. Tsuneyuki and H. Nishihara, *Chem. Sci.*, 2011, **2**, 1960-1968.
62. D. Streich, M. Karnahl, Y. Astuti, C. W. Cady, L. Hammarström, R. Lomoth and S. Ott, *Eur. J. Inorg. Chem.*, 2011, **2011**, 1106-1111.
63. E. J. Miller, T. B. Brill, A. L. Rheingold and W. C. Fultz, *J. Am. Chem. Soc.*, 1983, **105**, 7580-7584.
64. R. Xi, M. Abe, T. Suzuki, T. Nishioka and K. Isobe, *J. Organomet. Chem.*, 1997, **549**, 117-125.
65. G. Moula, M. Bose, B. K. Maiti and S. Sarkar, *Dalton Trans.*, 2012, **41**, 12926-12935.
66. D. Coucouvanis, E. D. Simhon, P. Stremple, M. Ryan, D. Swenson, N. C. Baenziger, A. Simopoulos, V. Papaefthymiou, A. Kostikas and V. Petrouleas, *Inorg. Chem.*, 1984, **23**, 741-749.
67. D. Coucouvanis, S. A. Al-Ahmad, A. Salifoglou, V. Papaefthymiou, A. Kostikas and A. Simopoulos, *J. Am. Chem. Soc.*, 1992, **114**, 2472-2482.
68. R. H. Herber, R. B. King and G. K. Wertheim, *Inorg. Chem.*, 1964, **3**, 101-107.
69. M. Itazaki, M. Ito, S. Nakashima and H. Nakazawa, *Dalton Trans.*, 2016, **45**, 1327-1330.
70. J. F. Moulder and J. Chastain, *Handbook of x-ray photoelectron spectroscopy : a reference book of standard spectra for identification and interpretation of XPS data*, Perkin-Elmer Co., Physical Electronics Division, 1992; p 261.
71. M. E. Ahmed, S. Dey, B. Mondal and A. Dey, *Chem. Commun.*, 2017, **53**, 8188-8191.
72. J.-F. Capon, F. Gloaguen, P. Schollhammer and J. Talarmin, *J. Electroanal. Chem.*, 2004, **566**, 241-247.
73. G. A. N. Felton, A. K. Vannucci, J. Chen, L. T. Lockett, N. Okumura, B. J. Petro, U. I. Zakai, D. H. Evans, R. S. Glass and D. L. Lichtenberger, *J. Am. Chem. Soc.*, 2007, **129**, 12521-12530.
74. J. Chen, A. K. Vannucci, C. A. Mebi, N. Okumura, S. C. Borowski, M. Swenson, L. T. Lockett, D. H. Evans, R. S. Glass and D. L. Lichtenberger, *Organometallics*, 2010, **29**, 5330-5340.

Graphical abstract

View Article Online
DOI: 10.1039/D0DT01428A

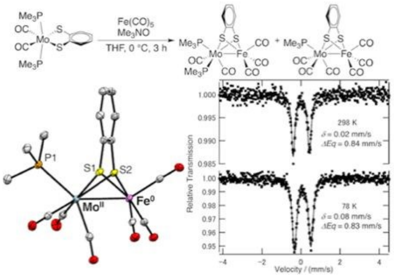

The benzenedithiolate-bridged MoFe complexes were synthesized and elucidated in the oxidation states of the metal centers.